

Brief Genetics Report

Fine-Mapping Gene-by-Diet Interactions on Chromosome 13 in a LG/J × SM/J Murine Model of Obesity

Thomas H. Ehrich,¹ Tomas Hrbek,¹ Jane P. Kenney-Hunt,¹ L. Susan Pletscher,¹ Bing Wang,¹ Clay F. Semenkovich,² and James M. Cheverud¹

Obesity is one of the most serious threats to human health today. Although there is general agreement that environmental factors such as diet have largely caused the current obesity pandemic, the environmental changes have not affected all individuals equally. To model gene-by-environment interactions in a mouse model system, our group has generated an F₁₆ advanced intercross line (AIL) from the SM/J and LG/J inbred strains. Half of our sample was fed a low-fat (15% energy from fat) diet while the other half was fed a high-fat (43% energy from fat) diet. The sample was assayed for a variety of obesity- and diabetes-related phenotypes such as growth rate, response to glucose challenge, organ and fat pad weights, and serum lipids and insulin. An examination in the F₁₆ sample of eight adiposity quantitative trait loci previously identified in an F₂ intercross of SM/J and LG/J mouse strains reveals locus-by-diet interactions for all previously mapped loci. *Adip7*, located on proximal chromosome 13, demonstrated the most interactions and therefore was selected for fine mapping with microsatellite markers. Three phenotypic traits, liver weight in male animals, serum insulin in male animals, and reproductive fat pad weight, show locus-by-diet interactions in the 127-kb region between markers *D13Mit1* and *D13Mit302*. The phosphofructokinase (PFK) C (*Pfkc*) and the pitrilysin metalloprotease 1 (*Pitrm1*) genes are compelling positional candidate genes in this region that show coding sequence differences between the parental strains in functional domains. *Diabetes* 54:1863–1872, 2005

From the ¹Department of Anatomy and Neurobiology, Washington University School of Medicine, St. Louis, Missouri; and the ²Department of Medicine, Washington University School of Medicine, St. Louis, Missouri.

Address correspondence and reprint requests to James M. Cheverud, Department of Anatomy and Neurobiology, Washington University School of Medicine, 660 S. Euclid Ave., St. Louis, MO 63110. E-mail: cheverud@wustl.edu.

Received for publication 15 September 2004 and accepted in revised form 18 February 2005.

Additional information for this article can be found in an online appendix at <http://diabetes.diabetesjournals.org>.

AIL, advanced intercross line; AUC, area under the curve; LOD, logarithm of odds; PFK, phosphofructokinase; QTL, quantitative trait locus; SNP, single nucleotide polymorphism.

© 2005 by the American Diabetes Association.

The costs of publication of this article were defrayed in part by the payment of page charges. This article must therefore be hereby marked "advertisement" in accordance with 18 U.S.C. Section 1734 solely to indicate this fact.

Estimates of the heritability of obesity in humans range as high as 70% based on twin studies (1). However, obesity in the developed world is increasing too rapidly to be caused by changes in genetic background (2). Moreover, some human genotypes are apparently resistant to an obesogenic environment and do not become obese (3). Genotype-by-environment interactions such as these have long been of concern to evolutionary biologists and have been commonly noted as important for evolutionary processes (4–6). Likewise, gene-by-diet interactions are known to influence obesity- and diabetes-related traits in humans (7–9).

The elucidation of the biochemistry of appetite control in mouse models generally depends on transgenic or knockout mice (7–8). Because of the complexity of the obese phenotype, it is unlikely that all gene-by-environment interactions will be discovered using these methods (9). Human studies examining gene-by-diet interactions rely on epidemiological data collected from large samples (10–12). While these and other studies make valuable contributions to our understanding of gene-by-diet interactions, large-scale human studies can be difficult due to unknown genetic lineages (13) as well as data collection biases (11).

With carefully controlled lineages and environments, samples derived from inbred mouse strains are amenable to powerful statistical dissection of complex genetic and environmental interactions (15). Crosses derived from the SM/J and LG/J mouse strains are particularly attractive for these types of studies. At 60 days of age, there is an ~24-g difference in weight between the two strains (16,17). Later experiments have demonstrated that this considerable weight difference is due to the many different genes of individually small effect (18). Furthermore, SM/J and LG/J respond differently to increased amounts of dietary fat (19,20).

To follow up on these earlier findings, we divided the 16th generation of an advanced intercross line (AIL) derived from SM/J and LG/J by diet, feeding half of the mice from each family a high-fat diet and the other half a low-fat diet. A quantitative genetic analysis of a number of obesity- and diabetes-related phenotypes, including growth rates, fat pad and organ weights, and serum levels of triglycerides, free fatty acids, cholesterol, and insulin,

TABLE 1
Composition of high- and low-fat diets

Component	High fat	Low fat
Energy from fat (%)	42	15
Casein (g/kg)	195	197
Sugars (g/kg)	341	307
Corn starch (g/kg)	150	313
Cellulose (g/kg)	50	30
Corn oil (g/kg)	—	58
Hydrogenated coconut oil (g/kg)	—	7
Anhydrous milk fat (g/kg)	210	—
Cholesterol (g/kg)	1.5	—
Kilojoules per gram	18.95	16.99

demonstrated that most traits, including fat pad weights, liver weight, and serum insulin, were heritable and genetically correlated (T.H.E., unpublished observations). All of these traits show a low cross-environmental correlation, indicating that different genes or gene effects are influencing the traits on the two diets and that dietary responses for these phenotypes are themselves heritable and genetically correlated (T.H.E., unpublished observations). Genetic variation for obesity- and diabetes-related traits and their dietary responses were also encountered in a set of recombinant inbred strains formed from the same parental strains (21).

Cheverud et al. (22) have previously mapped eight adiposity loci in an F_2 cross of SM/J and LG/J. The present study validates those QTLs in the F_{16} AIL and tests the current phenotypic trait suite for dietary response. One locus on chromosome 13 demonstrates a dietary response for a large number of traits. The region immediately around this locus has been fine mapped, and the results are presented here.

RESEARCH DESIGN AND METHODS

The sample used in this study is an F_{16} AIL (23) derived from SM/J and LG/J (WU:LG,SM-G14). The original SM/J (24) and LG/J (25) strains were selected in separate experiments for small and large 60-day body weight, respectively. Both strains of mice have been inbred for several decades (16). Parental mice were obtained from The Jackson Laboratory (Bar Harbor, ME). SM/J males were mated to LG/J females to produce an F_2 generation. Subsequent generations were maintained by quasi-random mating from the F_2 generation to the F_{16} generation. At least 65 mating pairs were used in each generation, with no sib mating, resulting in an effective sample size of ~300 for each generation (23). To generate the F_{16} animals, 71 pairs of F_{15} animals were double mated, resulting in an experimental F_{16} sample of 1,011 animals in 148 litters, with an average of 6.8 animals per sibship.

Animal husbandry and trait collection. Animals were housed with their mothers until 3 weeks of age, at which time each litter was separated into single-sex cages segregated by diet with no more than five animals per cage. The maternal diet was PicoLab Rodent Chow 20 (5053; Ralston Purina, St. Louis, MO), which derives 12% of its energy from fat. The composition of the high-fat diet (TD18337; Harlan Teklad, Madison, WI) and low-fat diet (D12284; Research Diets, New Brunswick, NJ) are shown in Table 1. All animals were fed ad libitum. The animal facility is on a 12-h light/dark cycle and maintained at a constant temperature of 21°C.

Animals were weighed once per week on the day of their birth from week 1 to week 20. Weights were divided into three growth periods: preweaning, postweaning, and adult. The preweaning growth period encompasses the time from 1 week of age until weaning at 3 weeks of age. The postweaning growth period extends from 3 to 10 weeks of age and is the main period of skeletal growth (19). The adult growth period consists of weeks 10–20, during which time most of the weight added is in the form of adipose tissue (19).

Many animals were subjected to a glucose tolerance test at 10 and 20 weeks of age as time permitted. This subset included animals from 95 litters and 78 sibships, with 217 female animals, of which 113 were fed a low-fat diet and 104 were fed a high-fat diet, and 213 male animals, of which 103 were fed

a low-fat diet and 110 were fed a high-fat diet. The protocol used has been described elsewhere (20). Briefly, a fasting glucose level was obtained followed by intraperitoneal injection of 0.01 ml of a 10% glucose solution for every gram of body weight. Further glucose readings were obtained over the course of the 2-h study and were used to calculate the area under the curve (AUC), an overall measure of the animal's glucose tolerance.

Following the 20-week glucose test, animals were killed and subjected to necropsy according to the protocol outlined by Ehrlich et al. (20). Briefly, animals were first fasted for 4 h and anesthetized by intraperitoneal injection of sodium pentobarbital. Serum samples were obtained via cardiac puncture followed by centrifugation and were then assayed for free fatty acids, triglycerides, cholesterol, and insulin. Organs (heart, liver, kidneys, and spleen) and fat pads (reproductive, renal, mesenteric, and inguinal) were removed and weighed. Detailed phenotypic data are available upon request.

Molecular mapping. Microsatellite markers chosen for this study come from the set developed for mouse gene mapping (26). Markers were chosen to cover the candidate regions as evenly as possible. Candidate markers have been tested to ensure polymorphism between LG/J and SM/J, with polymorphic markers comprising ~40% of all markers tested. PCR protocols are standard for this lab and have been detailed elsewhere (22). Map distances were calculated using the Mapmaker 3.0b program (27,28). Increased genetic recombination in an F_{16} generation results in an approximately eightfold expansion of chromosome map distances relative to an F_2 generation when expressed in Haldane's centimorgans (23), allowing for gene mapping on a much finer scale than is possible using F_2 intercross design. Locations of microsatellite markers used in this study have been verified by examining the physical location of each marker in the Ensembl database (www.ensembl.org). Genetic mapping data are available upon request.

Statistical analysis

Replication. A previous study by Cheverud et al. (22) detected eight QTLs affecting adiposity in an F_2 cross of SM/J and LG/J through interval mapping (29). Adiposity was defined for the purposes of that study as the weight of the reproductive fatpad divided by the total body weight of the animal at time of necropsy (22). Replication of the adiposity QTL detected in the original study was tested in the present experimental sample in a manner similar to that described by Vaughn et al. (30). Briefly, a regression analysis is performed (31) with adiposity as defined in the original study as the dependent variable and genotype at each marker tested as the independent variable. Markers were selected on the basis of proximity to the original QTL (22) as well as proximity to adiposity QTLs detected in the F_{10} AIL (J.M.C., unpublished data). A QTL is considered to have replicated if the probability of no genetic effect on adiposity at the locus examined is <0.05 . Because the diet used in the original study (22) corresponds more closely to the low-fat diet used in the present study, only animals fed a low-fat diet have been considered for replication. Unlike the present study, some animals in the previous study had been bred before being killed (22). Therefore, QTLs that only mapped to one sex in the original study have been examined in both sexes in the present study.

Testing loci for interactions. An initial test of previously identified loci affecting adiposity in a SM/J \times LG/J F_2 intercross (22) for gene-by-diet interactions has been performed using the following ANOVA model (33) at each microsatellite marker locus:

$$Y_{ijkl} = \mu + \text{Genotype}_i + \text{Sex}_j + \text{Diet}_k + \text{Genotype}_i \times \text{Sex}_j \\ + \text{Genotype}_i \times \text{Diet}_k + \text{Sex}_j \times \text{Diet}_k + \text{Genotype}_i \times \text{Sex}_j \times \text{Diet}_k + e_{ijkl} \quad (1)$$

where μ is the mean and Y_{ijkl} is the measurement on the l th individual for genotype i and sex j , raised on diet k . The same traits and loci were also tested separately in males and females, using the following ANOVA model, in which all symbols are the same as above (33):

$$Y_{ikl} = \mu + \text{Genotype}_i + \text{Diet}_k + \text{Genotype}_i \times \text{Diet}_k + e_{ikl} \quad (2)$$

Fine mapping. Following selection of a region for fine mapping, QTL detection was performed with minor modifications according to the interval mapping method detailed by Cheverud et al. (22). Briefly, the probability of an animal being homozygous for SM/J or LG/J was calculated from the recombination rates between a given locus and the flanking marker genotypes using previously derived equations (34) and our own software (35). Additive genotype scores (X_a) were defined based on this probability: (-1) times the probability of an animal being homozygous SM/J at a given locus and $(+1)$ times the probability of being homozygous LG/J at that locus. At observed marker loci, additive genotype scores were then defined as (-1) , (0) , and $(+1)$ for homozygous SM/J, heterozygous, and homozygous LG/J, respectively. Similarly, dominance scores (X_d) were defined as $(+1)$ times the probability of an animal being heterozygous at a given locus, according to the calculations

described above. At observed marker loci, dominance scores were defined as (+1) for heterozygous and (0) for homozygous individuals.

Phenotypes were then regressed on genotypes every 2 cM, as calculated in the F_{16} ALL (23), along the region of interest using the Set and Correlation feature of Systat 10.0 (36). Regression coefficients are the estimates of the additive (a) and dominance (d) genotypic values if a trait maps to the tested locus (37). The QTL was defined as the locus at which the trait has the lowest probability of having occurred by chance, assuming no genotype-phenotype association. The probability was then transformed to a linear scale by taking the \log_{10} conversion of the inverse of the lowest probability. This transformation converted the mapping results to a scale similar to that obtained using logarithm of odds (LOD) scores based on maximum likelihood analysis (29). All traits were mapped in the entire experimental sample, as well as in the following subsamples: females, males, animals fed the low-fat diet, animals fed the high-fat diet, female animals fed the low-fat diet, female animals fed the high-fat diet, male animals fed the low-fat diet, and male animals fed the high-fat diet.

The region of interest was also scanned for interactions between diet and additive and dominance scores, controlling for sex (when both sexes were analyzed simultaneously), diet, and the main effects of the genotype. A significant interaction effect indicated that the effect of genotype at a given locus was dependent on the diet of the animal.

After loci had been detected, confidence regions were better resolved by statistically accounting for flanking markers in the analysis according to the composite interval mapping method proposed by Zeng (38). Significance has been calculated to correct for multiple comparisons as described previously (22,39). Briefly, the number of effective markers is calculated to account for linkage according to the following equation:

$$M_{\text{ef}} = M \left(1 - \left(\frac{(M-1)V_{\text{obs}}}{M^2} \right) \right) \quad (3)$$

where M_{ef} is the number of effective markers, M is the actual number of markers used in the study, and V_{obs} is the variance of the eigenvalues of a correlation matrix of the additive genotype scores of the markers used. The effective number of markers is then used to calculate a Bonferroni-corrected significance threshold that accounts for multiple comparisons (39). The Bonferroni-corrected 5% significance threshold for this study on mouse chromosome 13 is 0.009, and the 1% significance threshold is 0.002. When converted to LOD scores by calculating the \log_{10} of the inverse of the probability levels, significance thresholds are 2.06 and 2.76, respectively. Because only one chromosome was examined, no genome-wide significance threshold was calculated.

Sequencing. Analysis of the QTL revealed two positional candidate loci, both of which were completely sequenced. The 6-phosphofructokinase (PFK) isoenzyme C (*Pfkfb*) and pitrilysin metalloprotease one (*Pitrm1*) genes are both involved in metabolism. Preparation of DNA and sequencing of the *Pfkfb* and *Pitrm1* genes followed the same procedure.

Total genomic RNA was extracted from liver tissue that was flash-frozen in liquid nitrogen. An $\sim 3\text{-mm}^3$ portion of liver tissue was powdered in a liquid nitrogen-chilled mortar with a pestle. Finely powdered tissue was dissolved in 1.5 ml Trizol reagent, homogenized, and RNA was extracted following manufacturer protocol. RNA was extracted from liver tissue of six males each of the SM/J and LG/J strains. Extracted RNA was quantified on a spectrophotometer and standardized to a concentration of ~ 0.5 mg/ml.

cDNA was generated from mRNA using reverse transcription. Two master mixes were prepared and kept on ice at all times. The first master mix contained 10 μl total mRNA, 3 μl of 100 $\mu\text{mol/l}$ oligo dT₂₀ primer, and 12 μl RNase-free ddH₂O. The second master mix contained 5 μl of $10\times$ Stratascript buffer (500 mmol/l Tris-HCl, pH 8.3, 750 mmol/l KCl, and 30 mmol/l MgCl₂), 10 μl of 8 mmol/l dNTPs, 1 μl Stratascript MLV-reverse transcriptase (50 units/ μl), and 9 μl RNase-free ddH₂O per reaction. The two master mixes were combined, gently mixed, and incubated at 42°C for 90 min in a thermocycler. After the 90-min incubation period, the cDNA was used directly or frozen at -20°C for later use.

PCR amplification was performed on cDNA samples. Negative controls were performed for all reactions. PCR was performed in 25- μl reaction volumes containing 11.8 μl ddH₂O, 1.7 μl of 10 mmol/l MgCl₂, 2.5 μl of $10\times$ buffer (500 mmol/l Tris-HCl, pH 9.2, 160 mmol/l ammonium sulfate, 25 mmol/l MgCl₂, and 1% Tween 20), 2.5 μl of each primer (0.2 mmol each forward and reverse primer), 2.0 μl dNTP mix (200 mmol each dNTP), 3 units KlenTaqLA DNA polymerase, and 1 μl DNA template. Because of the complexity of the cDNA mixture and highly variable concentrations of different cDNA products, target cDNAs were amplified using a nested PCR procedure. A nested PCR consists of a first round of PCR followed by a second round of PCR of the unpurified PCR product with a new set of primers placed internally to those used in the first PCR. The temperature profile for both PCRs consisted of 1)

preheating at 68°C for 60 s, 2) denaturation at 93°C for 10 s, 3) annealing at 55–50°C for 35 s, 4) extension at 68°C for 5 min, and 5) a final extension at 68°C for 10 min. Steps 2–4 were repeated 25 times; in the first 9 cycles, the annealing temperature was decreased by 0.5°C until 50°C annealing temperature was reached. The *Pfkfb* gene transcript was amplified with an external primer pair, 5'-TGCTGAGTACGGGAGTGTCTGGC-3' and 5'-AGCGTGAGCTGGGTTTCATG-3', and then a nested primer pair, 5'-GGCGTCTCTACCTCTCATCATG-3' and 5'-GTGGTGATGGCAAGTGGTGTC-3'. The *Pitrm1* gene transcript was amplified with 5'-CTGGCCCCACGCTGGTCCATG-3' and 5'-AACTCAGACAGTTGGAGTTGGC-3', and then a nested primer pair, 5'-CCCACGCTGGTCCATG-3' and 5'-TTTCCTTCAGAGTTTGGCCAGTC-3'.

The product resulting from the last PCR was evaluated on a 1.2% agarose gel and then purified with Qiagen spin-columns. The product was sequenced from specifically designed primers on both the heavy and light strands. Sequencing reactions followed standard Perkin-Elmer Big Dye sequencing protocol for double-stranded cycle sequencing reactions. Sequences were determined on an MJ Research BaseStation automatic DNA sequencer. Sequencing primers included 5'-GTATGGTGGCTCCATTGACA-3', 5'-ATCACCTCCAGGACGAAGGT-3', 5'-AAGAGGAAACCAAGCAGTGC-3', and 5'-CGACCGCATTAAACAGTCAGC-3' for the *Pfkfb* gene. The *Pitrm1* gene transcript was sequenced with 5'-GATGGCGTCTGGAGCATGAG-3', 5'-GGTCAGGAAGCAGCTTGTCT-3', 5'-TGATCGGATTGAAGCTCTGCTT-3', 5'-ATGTGCTCCCTGACGACTCA-3', and 5'-GCGAGTGTGTCAGGACTGTC-3'. Two individuals per strain were completely sequenced and their sequences assembled. No within-strain polymorphism was identified. The strains were compared with each other and with the C57BL/J strain sequence available from Ensembl Mouse build 32. Alleles of LG/J and SM/J animals for both *Pfkfb* and *Pitrm1* genes have been deposited in GenBank under numbers AY779273 to AY779276.

The potential functional effects of single nucleotide polymorphisms (SNPs) for both *Pfkfb* and *Pitrm1* genes of LG/J and SM/J animals were analyzed using the program SIFT (40). This procedure classifies SNPs on a scale contrasting tolerated to deleterious mutations. General matrix change probabilities were also inferred from the BLOSSUM62 amino acid matrix. To investigate the distribution of these SNPs in other taxa, and to compare them with the SNPs observed in the LG/J and SM/J strains, we surveyed all available sequence data for *Pfkfb* and *Pitrm1* genes in vertebrates. GenBank was accessed on 9 January 2005, and multiple sequence alignment was performed using ClustalW (41). After aberrant sequences were removed from the set, we obtained an alignment of 112 sequences for *Pfkfb* and 10 sequences for *Pitrm1*. Aligned *Pfkfb* genes included the LG/J and SM/J strain sequences, a C57BL/6J reference strain sequence, and a phylogenetically wide spectrum of vertebrates including zebrafish, *Xenopus*, chicken, and a range of mammals including humans. For the *Pitrm1* gene, only mouse and human sequences were available.

RESULTS

Replication. Eight previously detected adiposity QTLs were reexamined in the present experimental sample using both an expanded set of traits as well as a low- and high-fat diet. The fat content of the low-fat diet used in this study corresponds most closely to the diet used in the study that identified the loci under examination (22). Because of this, there is an inherent bias against finding QTLs in animals fed a high-fat diet and a bias toward finding QTLs in animals fed a low-fat diet in this selection of genomic regions. Of the original eight QTLs affecting adiposity, five (*Adip2*, *Adip3*, *Adip5*, *Adip6*, *Adip7*, and *Adip8*) replicated with a probability of $\leq 5\%$ or less whereas two (*Adip1* and *Adip4*) did not. *Adip7* was nearly significant in the low-fat sample, with a probability of 0.09. Although *Adip7* did not replicate in the low-fat sample for adiposity as defined in the original study, it was significant for the weight of the reproductive fat pad in male animals ($P = 0.02$). When the high-fat sample was examined, *Adip7* replicated in female animals ($P = 0.01$). The two loci that did not replicate may have been due to tested markers missing the region of interest (see DISCUSSION). Of the QTLs that did replicate, two (*Adip3* and *Adip6*) did so with a probability < 0.01 . QTLs that replicated are indi-

TABLE 2
QTL replication and locus-by-diet interactions

Adiposity QTL	Chromosome	Markers tested	Replication probability	Traits significantly affected by locus-by-diet interactions
<i>Adip 1</i>	1	<i>D1Mit78</i>	0.139	10-week AUC(f), 20-week AUC(m), mesenteric/total fat(m)
<i>Adip 2</i>	6	<i>D6Mit14</i>	0.726	Renal fat(m), mesenteric fat, inguinal fat(m), triglycerides(m), total fat(m), renal/body(m), inguinal/body(m), reproductive/total(m), inguinal/total(m), adiposity(m)
<i>Adip 3</i>	7	<i>D6Mit58</i>	0.023	Postweaning growth, adult growth(m)
		<i>D7Mit148</i>	0.004	20-week AUC, adult growth, inguinal/body(m), mesenteric/body(m), adiposity(m)
<i>Adip 4</i>	8	<i>D7Mit17</i>	0.107	None
		<i>D8Mit56</i>	0.613	Free fatty acids(f), spleen(f), mesenteric/total(m)
<i>Adip 5</i>	9	<i>D8Mit324</i>	0.761	None
		<i>D9Mit8</i>	0.004	Renal fat, reproductive/body(m), reproductive/total(m)
<i>Adip 6</i>	12	<i>D9Mit19</i>	0.095	10-week basal glucose(f), insulin(f), liver(f)
<i>Adip 7</i>	13	<i>D12Mit5</i>	0.014	None
		<i>D13Mit1</i>	0.156	Insulin(m), liver(m), 20-week basal glucose(m), reproductive fat(m), total fat(m), reproductive/body(m)
<i>Adip 8</i>	18	<i>D13Mit115</i>	0.027	Insulin, kidney, reproductive fat, inguinal fat(f), total fat, heart(f), liver(f), triglycerides(m), insulin(m), reproductive/body, inguinal/body, reproductive/total(m), reproductive/total(f), adiposity
		<i>D18Mit51</i>	0.027	Free fatty acids(m)
		<i>D18Mit209</i>	0.027	None

Adiposity QTLs are taken from Cheverud et al. (22). Chromosomal location and markers chosen to test for replication and interactions are indicated. All QTLs with the exception of *Adip1* and *Adip4* replicated for at least one of the associated markers tested. All loci replicated in the sample were fed a low-fat diet with the exception of *Adip7*, which only replicated in female animals fed a high-fat diet. Traits that are significantly affected by diet-by-genotype interactions for each locus are shown in the right-hand column. Sex-specific effects are indicated by (f) for female-specific effects or (m) for male-specific effects.

cated in boldface in Table 2, and the probability associated with replication is indicated.

QTL-by-diet interactions. Because of the increased recombination in the F₁₆ AIL, two markers have been used for many of the QTLs to provide more complete coverage of the confidence region observed in the F₂ generation. Traits showing a significant locus-by-diet interaction are shown in Table 2. All of the QTLs with the exception of *Adip6* show a significant locus-by-diet interaction for at least one of the phenotypic traits examined. Of the loci examined, *Adip7* demonstrated a significant locus-by-diet interaction for the largest number of traits and so this locus on the proximal end of chromosome 13 was selected for further analysis by fine mapping.

Fine mapping. The following markers were chosen to saturate the *Adip7* region: *D13Mit1*, *D13Mit302*, *D13Mit300*, *D13Mit80*, *D13Mit172*, *D13Mit134*, *D13Mit207*, *D13Mit57*, *D13Mit115*, *D13Mit135*, *D13Mit163*, and *D13Mit84* according to the methods outlined above. Analysis of the recombination data in MapMaker 3.0b calculates a distance of 86 cM, which corresponds to 10.75 cM in F₂ units (23). On the Ensembl physical map, these markers cover the distance from 6.2 to 25.1 Mbp from the centromere of chromosome 13. Three of the markers initially scored, *D13Mit300*, *D13Mit172*, and *D13Mit57*, were uninformative due to lack of recombination with adjacent markers (*D13Mit302*, *D13Mit80*, and *D13Mit207*, respectively) and so were dropped from the analysis.

QTLs detected are shown in Fig. 1. Horizontal lines represent the LOD values for the trait listed over the 1-LOD drop confidence region. The peaks of these curves represent the most likely location for the QTL mapped. As

can be seen in Fig. 1A, when animals fed both diets are considered together, QTLs for seven traits clustered in two regions along the chromosome are significant. The postweaning growth period among female animals occupies a large confidence region, from midway between *D13Mit1* and *D13Mit302* to midway between *D13Mit134* and *D13Mit207* with an LOD score of 2.2. This region overlaps with the QTL for 10-week AUC, which is highly significant with an LOD score of 4.1. The confidence interval for the QTL for 10-week AUC also occupies a much smaller area of the region mapped, ~1.5 F₂ cM around *D13Mit134*.

All other significant QTLs occupy the region from *D13Mit207* to *D13Mit163*, the most distal marker considered in this study. These traits include the inguinal fat pad in male animals, heart weight, 20-week AUC in male animals, and spleen weight. A QTL for postweaning growth phase is also in this region. This differs from the more proximal QTL for the same trait in that this QTL is for both sexes considered together, rather than only female animals.

Locus-by-diet interactions. As can be seen from a comparison of Fig. 1B and Fig. 1C, the pattern of QTLs detected differs dramatically based on which diet is considered. The four QTLs detected in animals fed a high-fat diet fall into two groups along the region of interest, as shown in Fig. 1B. The confidence interval for liver weight in male animals occupies a region running from *D13Mit1*, the most proximal marker considered, to midway between *D13Mit302* and *D13Mit134*. The LOD score for this trait is significant with an LOD of 2.3. The other traits detected, 20-week AUC in male animals, serum triglyceride levels in male animals, and mesenteric fat pad-to-body weight

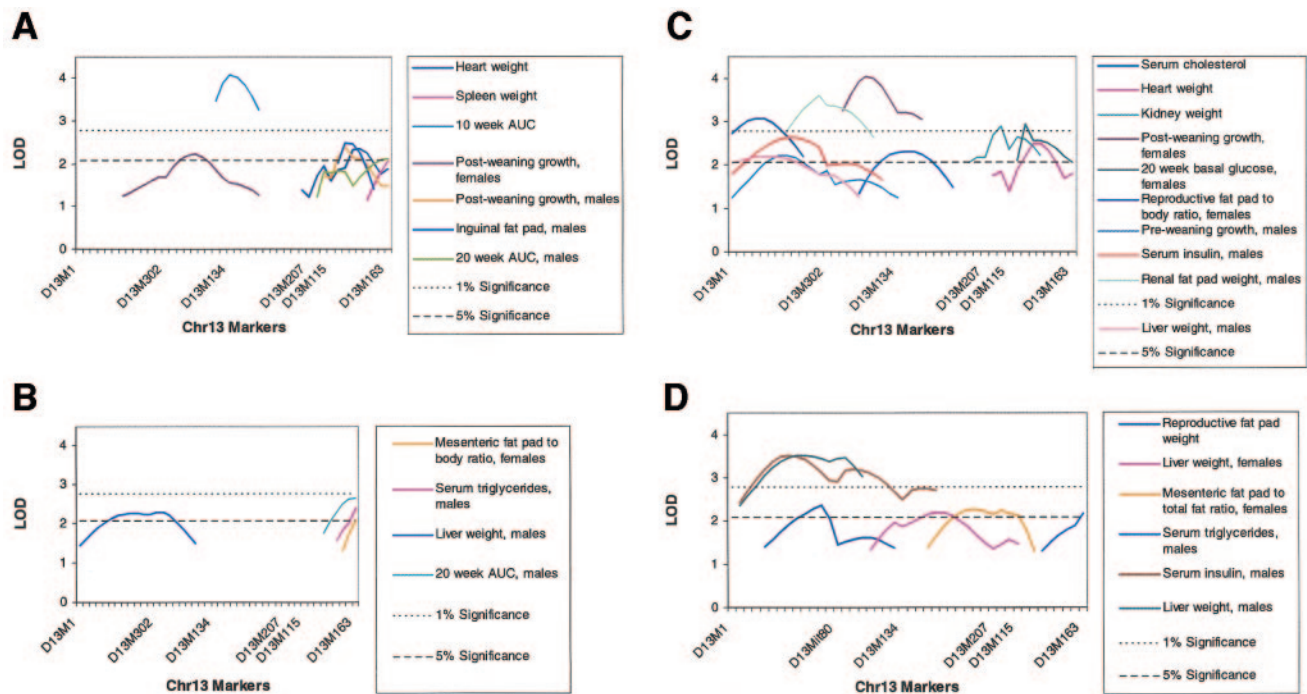


FIG. 1. QTLs are indicated by phenotype and grouped by samples included in the analysis: both diets (A), the high-fat-fed animals (B), the low-fat-fed animals (C), and locus-by-diet interaction (D). Location along chromosome 13 is indicated by marker identity. Tick marks along the x-axis indicate 2-cM intervals in F_2 Haldane's centimorgan units. QTL effects are indicated by lines plotting the LOD score for each phenotype and extending across the 1-LOD drop confidence interval for each phenotype.

ratio in female animals all occupy a relatively small region near the distal end of the region of interest, around *D13Mit163*. The significance region for these traits extends beyond the region fine mapped in the present study. This region in the high-fat diet subsample corresponds to the distal region containing five significant traits when both diets are considered together. One trait, 20-week AUC in male animals, is significant when both diets are analyzed together as well as in the high-fat sample. Because the LOD score for this trait is higher in the sample of male animals fed a high-fat diet than in the total male sample, and because the QTL for this trait is not significant when male animals fed a low-fat diet are considered, the effect seen in the total sample of male animals derives from male animals fed a high-fat diet. None of the traits detected in the sample of animals fed a high-fat diet are significant at a 1% level.

In contrast to the relatively small number of traits detected in the sample of animals fed a high-fat diet, QTLs representing 10 traits spanning the entire region of interest were detected in the sample of animals fed a low-fat diet, as shown in Fig. 1C. As previously noted, the study design is biased to detect traits in animals fed a low-fat diet because that is how the locations for further study were chosen, which may account for the greater number of QTLs detected in the low-fat-fed sample. Of special interest is the QTL for liver weight in male animals, which overlaps with the QTL for the same trait detected in the sample of animals fed a high-fat diet (Fig. 1B). However, the QTL for this trait is not significant when both diets are considered together (see Fig. 1A), indicating that this region has opposite effects depending on which dietary treatment is considered.

A comparison of the QTL for the postweaning growth

phase in female animals fed a low-fat diet versus the same trait for all female animals considered together indicates that the effect detected with both diets is due almost entirely to the low-fat-fed sample. The QTL for postweaning growth phase among female animals is highly significant in this sample, with a high LOD score of 4.0. The confidence region for this QTL, from slightly distal of *D13Mit302* to slightly distal of *D13Mit134*, overlaps the confidence region for the same trait in Fig. 1A. Because the QTL for this trait is not significant for the subsample of female animals fed a high-fat diet, and because the LOD score of the subsample of female animals fed a low-fat diet is higher than that of the total female sample, the effect seen in the total female sample is due to the subsample of female animals fed a low-fat diet. A similar pattern is true of the QTL for heart weight, which is more strongly significant when only the subsample of animals fed a low-fat diet is considered (LOD 2.5) than when the total sample of animals is considered (LOD 2.3) and is not significant in the subsample of animals fed a high-fat diet.

Figure 1D shows QTLs for gene-by-diet interactions. Rather than mapping a trait per se, this analysis considered the difference in effect between animals fed a low-fat diet versus animals fed a high-fat diet, as described in the statistical analysis above. These are QTLs for dietary response. A total of six significant dietary response QTLs have been detected in this region. The three most proximal QTLs, occupying the region from *D13Mit1* to midway between *D13Mit134* and *D13Mit207*, are also the traits of this set with the highest LOD scores. The QTL for serum insulin in male animals, with an upper LOD score >3.5, is highly significant when the interaction between genotype and diet is considered. The same trait is significant when the subsample of male animals fed a low-fat diet is

considered, but not at the same level (LOD 2.6), and the QTL for this trait is not significant in either the subsample of male animals fed a high-fat diet or the total sample of male animals.

The QTL for liver weight in male animals is not significant when all male animals are considered together, but, as noted above, is significant when either dietary subsample is considered separately. This indicates that this region of the genome has opposite effects on liver weight in male animals, depending on which diet the animal is fed. This is also shown in Fig. 1D. With an LOD score of 3.5, the QTL for the interaction effect on liver weight in male animals is more significant than in either dietary subsample.

The QTL representing the ratio of the weight of the mesenteric fat pad in female animals when considered as a percentage of the total amount of fat removed from the animal shows significant locus-by-diet interaction, corresponding to the region in the low-fat subsample with reproductive fat pad-to-body weight ratio. Liver weight among female animals also shows a significant interaction effect in this region. Finally, serum triglycerides show a significant interaction effect in the distal part of the region of interest.

Figure 2 shows the effect of genotype on dietary response traits with the highest LOD scores: serum insulin levels in male animals, liver weight in male animals, and reproductive fat pad weight. In all cases, the effects of genotype and diet are examined at the locus with the highest LOD score for each trait. As shown in Fig. 2A, an animal that is SM homozygous at *D13Mit1 + 1.5* F₂ cM averages ~1.95 ng/ml serum insulin at time of necropsy if fed a low-fat diet since weaning. When an animal with the same genotype at this locus has been fed a high-fat diet, it averages 8.34 ng/ml of serum insulin at time of necropsy, presumably following a well-established pattern of increased serum insulin in response to decreased insulin sensitivity after prolonged exposure to a high-fat diet. Animals that are heterozygous at this locus and have been fed a low-fat diet have slightly higher levels of serum insulin (2.23 ng/ml) than SM/J homozygotes at this locus that have been fed a low-fat diet, while *D13Mit1 + 1.5*-cM heterozygotes fed a high-fat diet have somewhat lower levels of serum insulin (7.55 ng/ml) than comparably fed SM/J homozygotes. When animals that are LG/J homozygous at this locus are considered, the difference between the two diets almost disappears: animals of this genotype fed a low-fat diet have much higher levels of serum insulin (4.03 ng/ml), whereas animals that are LG/J homozygous at this locus that have been fed a high-fat diet have only slightly increased levels of serum insulin (5.13 ng/ml).

In summary, the difference in serum insulin levels between animals fed the low-fat versus the high-fat diet is highly contextual, depending strongly on the underlying genotype at *D13Mit1 + 1.5*. The diet-based difference varies from 6.39 ng/ml for SM/J homozygotes at this locus, to 5.32 ng/ml for heterozygotes, and down to 1.10 ng/ml for LG/J homozygotes. This is a locus-by-diet interaction and indicates that the effect of a genotype at this locus on the serum insulin level of the animals is strongly dependent on the diet the animal consumes.

A similar phenomenon occurs with liver weight at nearly the same genomic position: the difference in liver weight between two male animals that are both homozygous SM/J

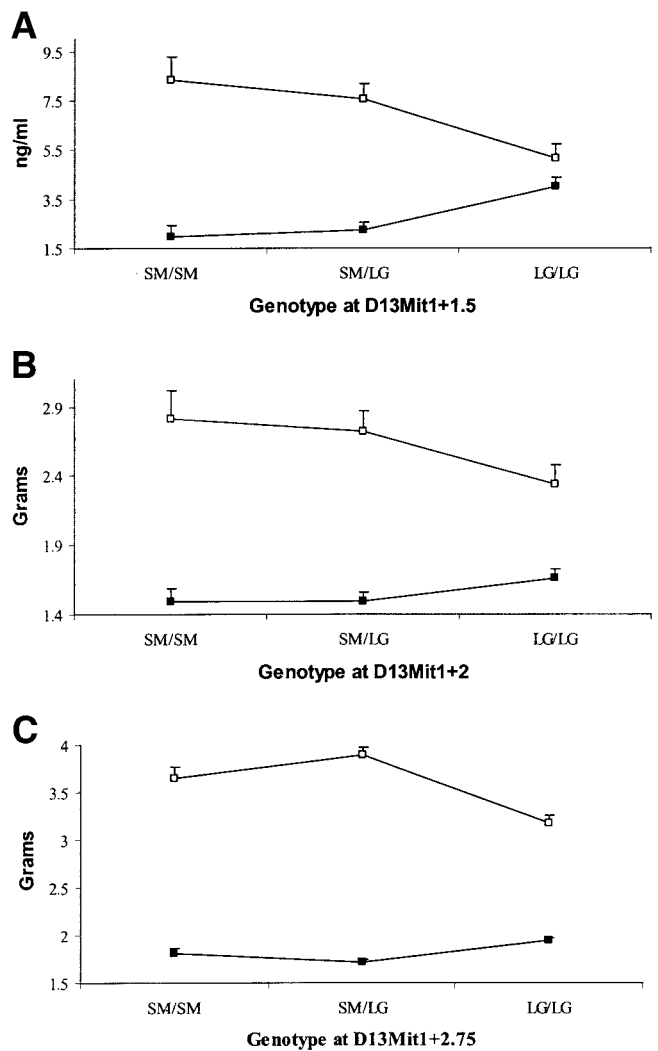


FIG. 2. Genotypic values for diet by locus interactions on proximal chromosome 13. The effect of a genotype on serum insulin in male animals (A), liver weight in male animals (B), and reproductive fat pad (C) are shown. ■, low-fat-fed animals; □, high-fat-fed animals. Upper error bars are indicated. Specific locus is indicated in the figure.

at *D13Mit1 + 2* F₂ cM but fed a low-fat versus high-fat diet is 1.32 g, versus only 0.67 g for male animals that are homozygous LG/J at this locus but fed a low-fat versus high-fat diet. Figure 2C shows the interaction of locus *D13Mit1 + 2.75* F₂ cM with diet in affecting the weight of the reproductive fat pad. The overall pattern is similar to the above two cases in that there is a greater response to dietary fat in animals that are homozygous SM/J at this locus than in animals that are homozygous LG/J.

Genomic region. The focus of this study is on possible gene-by-diet interactions, as opposed to genetic effects on both diets or on a high- or low-fat diet separately. The highest LOD peaks for gene-by-diet interactions occur between *D13Mit1* and *D13Mit134*, as shown in Fig. 1D. Table 3 shows the known and putative transcripts located between these markers according to Build 32 (1 April 2004) of the Ensembl database. Microsatellite markers used to fine map the interaction effects are shown in bold italics, with F₂ cM distances indicated.

The region of interest for the locus-by-diet interaction fine mapping corresponds to the short arm of human

TABLE 3
Positional candidate genes located between *D13Mit1* and *D13Mit134*

Gene	Start	Stop
<i>D13Mit1</i> (<i>D13Mit1</i> + 0 cM)	6,217,175	
<i>D13Mit302</i> (<i>D13Mit1</i> + 3.00 cM)	6,344,138	
<i>Pitrm1</i>	6,360,469	6,392,544
<i>Pfkip</i>	6,392,256	6,460,617
<i>Tubb2</i>	6,649,117	6,651,880
<i>D13Mit80</i> (<i>D13Mit1</i> + 3.25 cM)	8,858,870	
<i>3110035P10Rik</i>	8,905,602	8,971,735
<i>Idi1</i>	8,986,339	8,991,445
<i>4833405L16Rik</i>	9,075,125	9,081,660
<i>4833405L16Rik</i>	9,137,528	9,145,600
<i>Gtpbp4</i>	9,157,124	9,180,677
<i>AI256361</i>	9,278,546	9,355,769
<i>NM_172459</i>	9,796,143	9,851,686
<i>2900024P20Rik</i>	9,853,202	9,854,579
<i>2210402G22Rik</i>	9,920,581	10,000,960
<i>Chrm3</i>	10,116,058	10,117,827
<i>D13Mit134</i> (<i>D13Mit1</i> + 5.25 cM)	12,165,106	

All information presented in this table is from Build 32 (1 April 2004) Ensembl database (www.ensembl.org). Microsatellite markers used in fine mapping are indicated in bold italics, with the distance from *D13Mit1* shown in F_2 cM immediately below. Genes and putative genes are indicated in italics. While the 5% confidence region for the interaction effects shown in Fig. 1 lies between *D13Mit1* and *D13Mit134*, the LOD peaks for these effects are closest to *D13Mit302*.

chromosome 10. The actual LOD peaks all are immediately distal to *D13Mit302*. A search of this region yields two known genes, either or both of which are positional candidate genes that may contribute to the genotype-by-diet differences observed in this study. The first is a ptilinysin (*Pitrm1*; Ensembl ID ENSMUSG00000021193; GenBank AF513714 and NM_145131) and the second is 6-phosphofructokinase isozyme C (*Pfkip*; Ensembl ID ENSMUSG00000021196; GenBank AF123533).

The *Pfkip* gene codes for a 6-PFK that catalyzes the transfer of a phosphate residue from ATP to fructose-1-P to form fructose 1,6-P₂ (42). Enzymes in the PFK family are the rate-limiting step in the metabolism of pyruvate from hexose phosphate (rev. in 42). A detailed sequence analysis of the SM/J and LG/J alleles, and their comparison with the C57BL/6J allele, is shown in Table 4. The SM/J allele differs from the LG/J allele at 15 sites. Of these 15 sites, 5 result in putative amino acid differences, while the

TABLE 4
Pfkip gene

Position	129	201	782	849	874	1050	1281	1704	2028	2031	2046	2082	2310	2329	2345
C57BL	C	G	G	C	G	A	C	A	A	G	G	G	T	T	A
LG/J	C	A	A	T	A	C	T	G	G	T	A	C	C	C	G
SM/J	T	G	G	C	G	A	C	A	A	G	G	G	T	T	A
Codon	3	3	2	3	1	3	3	3	3	3	3	3	3	1	2
AA	R-R	V-V	R-Q	I-I	V-M	A-A	A-A	S-S	A-A	P-P	R-R	E-D	S-S	S-P	E-G
Prob	5	4	1	4	-2	4	4	4	4	7	5	2	4	-1	-2
SIFT			0.10		0.03*							0.53		0.15	0.27

Position represents a base pair position from the 5' end of the *Pfkip* gene. Sequence data from C57BL/6J mouse are from Ensembl Mouse Build 32. Codon signifies which codon the respective position represents, and AA signifies resulting amino acid change, if any. Prob signifies the log₁₀ odds of amino acid changes derived from the BLOSUM62 matrix. SIFT signifies probabilities of amino acid changes having a significant deleterious effect. *Statistical significance at the 5% level. Amino acid changes between LG/J and SM/J mice are highlighted in bold.

remaining 10 sites are silent, i.e., at degenerate positions. In comparison with the C57BL/6J allele, the SM/J allele shows no difference in amino acid composition and differs by only one silent transition at position 129. The LG/J allele differs from the C57BL/6J allele at 14 nucleotides, 9 of which are silent mutations, with the remaining 5 mutational differences resulting in five putative amino acid changes. Associated log₁₀ odds of specific amino acid changes derived from the BLOSUM62 matrix are shown in Table 4 along with the probability of tolerated functional effects at those locations derived using the SIFT algorithm (40). Transitional probabilities <0.05 are considered to have a significantly deleterious effect.

Briefly, in order of least to most likely amino acid changes in this protein are the replacement of valine with methionine at amino acid 292 (change at nucleotide 874), arginine with glutamine at position 261 (nucleotide 782), serine with proline at position 777 (nucleotide 2329), glutamic acid with glycine at position 782 (nucleotide 2345), and glutamic acid with aspartic acid at position 694 (nucleotide 2080). The valine-to-methionine replacement in the LG/J mouse strain is predicted to have a significantly deleterious effect ($P = 0.03$), although change in these residues represents a relatively small structural change from medium to large nonpolar amino acid. An analysis of 112 sequences deposited in GenBank indicated that amino acid mutations at this position are very rare across taxa and across *Pfkip* gene paralogues. Only the zebrafish had the amino acid threonine at this position, while all other vertebrates including all human and nonhuman primates had valine. The arginine-to-glutamine replacement ($P = 0.10$) does not appear to be significantly deleterious; however, this replacement represents a relatively large structural change due to a replacement of a medium-large polar amino acid by a medium-small polar amino acid. This mutation is also rare, with only the zebrafish (alanine), chicken (glycine), and rabbit (glutamine) deviating from the common amino acid (arginine) found in all other vertebrates including all human and nonhuman primates. Together with the valine-to-methionine replacement ($P = 0.03$), the arginine-to-glutamine change ($P = 0.10$) is likely to have the greatest functional effect.

Functionally divergent changes also include the glutamic acid-to-glycine ($P = 0.27$) and serine-to-proline ($P = 0.15$) transitions that result in small polar to small nonpolar and small nonpolar to small polar changes, respectively. The close proximity of these amino acid

TABLE 5
Pitrm1 gene

Position	44	50	55	513	631	632	634	1005	1383	1384	1637	1747	2328	2610	2895
C57BL	G	G	G	C	G	T	A	G	T	G	C	A	C	G	T
LG/J	<i>A</i>	<i>T</i>	<i>T</i>	T	<i>A</i>	<i>C</i>	<i>G</i>	A	C	A	A	G	T	A	C
SM/J	<i>A</i>	<i>T</i>	<i>T</i>	C	<i>A</i>	<i>C</i>	<i>G</i>	G	T	G	C	A	C	G	T
Codon	2	2	1	3	1	2	1	3	3	1	2	1	3	3	3
AA	<i>R-Q</i>	<i>S-I</i>	<i>G-C</i>	C-C	<i>V-T</i>	<i>V-T</i>	<i>N-D</i>	P-P	P-P	V-M	T-K	I-V	N-N	R-R	P-P
Prob	1	-2	-3	9	-2	-2	1	7	7	-2	0	1	6	5	7
SIFT										0.01*	0.21	0.47			

Position represents a base pair position from the 5' end of the *Pfkfb* gene. Sequence data from C57BL/6J mouse are from Ensembl Mouse Build 32. Codon signifies which codon the respective position represents, and AA signifies resulting amino acid change, if any. Prob signifies the log₁₀ odds of amino acid changes derived from the BLOSUM62 matrix. SIFT signifies probabilities of amino acid changes having a significant deleterious effect. *Statistical significance at the 5% level. Amino acid changes between LG/J and SM/J mice are highlighted in bold. Amino acid changes between C57BL and LG/J + SM/J mice are in bold italics; these mutational changes result in no differences between LG/J and SM/J mice. Mutations at site 631 and 632 both contribute to the change from valine to threonine.

residues and the parallel but opposite changes in their polarities may result in functional compensation. Additionally, these amino acids are located at the COOH-terminus of the protein and are therefore less likely to be of functional significance. This hypothesis is supported by an observation of large variation in amino acid composition at the COOH-terminus among vertebrate taxa. The glutamic acid to aspartic acid replacement is expected to have little effect ($P = 0.53$).

The *Pitrm1* gene plays a critical role in energy production in mitochondria. It is involved in the processing and degradation of NH₂-terminus presequence peptides of other nuclear-encoded mitochondrial genes as they enter the mitochondrial matrix through the lipid membrane. Failure to degrade these peptides is toxic for the mitochondria. Together with ATP-dependent and other metal-dependent proteases, *Pitrm1* functions as a quality control gene of the mitochondrial inner membrane. Through its quality control role, it regulates mitochondrial functionality and efficiency in energy production.

We also examined sequence variation in the *Pitrm1* gene (Table 5). The LG/J mice differ from SM/J mice at nine nucleotide positions, three of which result in amino acid changes. Both LG/J and SM/J differ from C57BL/6J mice at an additional six nucleotide positions, all of which result in amino acid changes. However, two of those positions are adjacent and part of the same putative amino acid; thus, the six nucleotide differences result in only five amino acid changes. The change from valine to methionine at position 462 (nucleotide 1384) has a low probability and most likely results in a strong functional effect ($P = 0.01$). All sequences deposited in GenBank contain valine at amino acid position 462, but only the LG/J mice contain methionine at this position. The two other amino acid changes observed between LG/J and SM/J mice represent relatively common changes and would appear to have nonsignificant functional effects. At amino acid position 546 (nucleotide 1637), threonine in SM/J mouse is replaced by lysine in LG/J mouse with nonsignificant functional effect ($P = 0.21$), while at position 583 (nucleotide 1747) a functionally nonsignificant ($P = 0.47$) transition from isoleucine to valine is observed.

DISCUSSION

This study utilizes an F₁₆ AIL segregated by diet to map gene-by-diet interactions in previously identified adiposity

QTLs. Of the previously identified adiposity QTLs, five of the original eight replicated at the 5% level or better. Two of the previously identified adiposity QTLs did not replicate. However, the lack of replication may be explained by discrepancies in the genetic maps used for each study. The 2001 study relied on recombinational mapping to determine marker position (22), and markers were chosen for the genome-wide scan on the basis of F₁₀ recombinational data (data not shown). Subsequent examination of the Ensembl physical database (www.ensembl.org) reveals that the marker chosen to replicate *Adip1*, *DIMit178*, is actually centromeric of its original apparent map position. Examination of other experimental samples derived from the same parental cross by our group has replicated *Adip1* (data not shown). Similarly, the markers chosen to replicate *Adip4*, *D8Mit56* and *D8Mit324*, are telomeric of the original QTL position (data not shown).

Seven of the eight previously detected QTLs (*Adip1*, -2, -3, -4, -5, -7, and -8) demonstrated locus-by-diet interactions for a large series of obesity- and diabetes-related traits. These include a variety of fat pads, responses to glucose challenge, organ weights, and serum plasma levels of insulin, triglycerides, and free fatty acids. These collective results indicate that adiposity QTLs also affect dietary responses, in that the LG/J and SM/J alleles are differentially sensitive to a high-fat diet. Most often (60% of the time) SM/J homozygotes at these QTLs are more responsive to a high-fat diet than LG/J homozygotes. This is especially true for *Adip3*, -5, -7 and -8. In contrast, LG/J homozygotes at *Adip2* and -4 are more sensitive to dietary fat than SM/J homozygotes.

When animals fed both a low- and high-fat diet are considered together, a number of additional phenotypes map to *Adip7*, the adiposity QTL on chromosome 13. These include postweaning growth in female animals, 10-week AUC, and 20-week AUC in male animals. However, more striking are the differences between the QTLs detected among animals fed a low-fat diet and those fed a high-fat diet. In some cases, such as with postweaning growth among female animals and 20-week AUC among male animals, it becomes apparent that the overall effect is due only to half of the sample assayed: one sex is affected while the other is not. Other phenotypes, such as serum triglycerides in male animals fed a high-fat diet and renal fat pad weight in male animals fed a low-fat diet, are observable only in one dietary subsample, but not the

other. The LOD peaks in the subsample fed a high-fat diet for 20-week AUC in males, serum triglycerides in males, and mesenteric fat pad-to-body weight ratio in females all occur distally of the region fine mapped in this study, and further analysis will be needed to determine the location of the actual peaks for these traits. Perhaps most intriguingly, the QTL for liver weight among male animals is significant in both dietary subsamples considered separately, but not together.

This mystery is resolved when the difference between traits on different diets, or dietary responses, are mapped rather than the traits themselves. The interaction between locus and diet affecting liver weight among male animals, for example, has an LOD of 3.5, which is higher than the main effect in either dietary subsample. The QTL for serum insulin in male animals is not significant in animals fed a high-fat diet, is significant at the 5% level in animals fed a low-fat diet, but is significant well above the 1% level when considered as an interaction.

For both serum insulin and liver weight, the locus-by-diet interaction effect is caused by a difference in magnitude of effect: SM/J homozygous animals respond more strongly to higher levels of dietary fat than do LG/J homozygous animals. In both cases, heterozygous animals fall somewhere between the homozygotes, although SM/J is partially dominant to LG/J with respect to dietary response. Reproductive fat pad weight also shows a difference of magnitude of response to diet dependent on genotype, although it also seems to show some degree of overdominance, since the degree of difference between the two diets is greatest among animals that are heterozygous at the locus examined. Serum triglyceride levels in male animals also show a gene-by-diet interaction at the distal end of the region examined, and a distal extension of fine-mapping efforts will be necessary to elucidate the locus for this effect.

Liver weight in male animals and serum insulin levels in male animals showed the strongest gene-by-diet interactions as measured by LOD interaction scores in Fig. 1D. The peaks for both of these traits occur between *D13Mit1* and *D13Mit134*, and a preliminary gene scan was performed in this region, which comprises ~6 million bp. Although identification of the genes involved in the different dietary responses is an ongoing process, two promising potential candidate genes were located in the dietary response QTL support interval on chromosome 13: the *Pfkfb* gene and the *Pitrm1* gene.

The *Pfkfb* gene plays a crucial role in metabolism as the rate-limiting and most commonly regulated step in glycolysis. The PFK family of enzymes (EC 2.7.1.11) catalyzes one of the rate-limiting steps in the formation of pyruvate in mammalian cells: the phosphorylation of fructose-6-phosphate to fructose 1,6-bisphosphate in an MgATP-dependent manner (43). Different isozymes of PFK form both homo- and heterodimers, allowing for a range of regulatory function (43). In fact, there is some evidence that the human form of the C isozyme identified in this study plays a primarily regulatory role in ascites tumors by regulating the activity of other PFK isozymes (44). The *Pfkfb* gene has five amino acid differences between the SM/J and LG/J alleles, two of which have potentially important functional effects.

The valine-to-methionine replacement at amino acid position 292 has been identified as the most likely functionally deleterious mutation. The arginine-to-glutamine replacement at amino acid position 261 has a lower probability of functional effect but structurally presents a relatively large change because of the replacement of a medium-large polar amino acid by a medium-small polar amino acid. Both of these positions lie in highly conserved regions and are mutations that might potentially cause secondary and tertiary conformational changes, affecting the specificity of regulatory binding sites. Unfortunately, no three-dimensional structure for eukaryotic PFK enzymes exists, so there is no way, at present, to examine this possibility with certainty.

We can speculate on the possible role of PFK in response to a high-fat diet. Given the contextual relationship between genotype, diet, and the phenotype of increased fat pad/liver weight/hyperinsulinemia, the mice with SM/J genotypes likely manifest accelerated deposition of fat in adipose tissue (reproductive fat depot) when challenged with a high-fat diet. Increased adiposity can alter the secretion of adipokines, such as adiponectin (45), leading to insulin resistance. In an effort to maintain normal circulating glucose levels, the pancreatic β -cell compensates for insulin resistance by secreting more insulin, resulting in hyperinsulinemia. Insulin resistance is commonly associated with fatty liver, perhaps related to enhanced delivery of free fatty acids from fat stores to the liver (46), thus the effect on liver weight. While the mechanisms by which these candidate genes affect dietary response are speculative, there is previous evidence supporting a potential role for PFK in mediating weight gain in response to high-fat feeding in rodents (47).

Pitrm1 is related to the insulin-degrading enzyme and other peptide processing enzymes. It removes presequence mitochondrial targeting peptides, which serve an important role in moving peptides from the cytosol into the mitochondrial matrix. If these targeting peptides are not removed, they can be toxic to the mitochondrion and thus could affect mitochondrial activity. It has recently been suggested that impaired mitochondrial activity may play an important role in insulin resistance and diabetes (48–51). The *Pitrm1* alleles found in the SM/J and LG/J mice show functionally important differences at five amino acids when compared with C57BL/6J mice. However, there are only three amino acid differences observed between the SM/J and LG/J alleles. Of these three mutations, the amino acid change from valine in SM/J mice to methionine in LG/J mice at amino acid 462 is the most likely to have a functional effect ($P = 0.01$). The amino acid methionine is clearly the aberrant residue, since human sequences also contain valine at position 462.

Pitrm1 is probably required for the normal processing of peptides by mitochondria, and defects in its function could disrupt mitochondrial function. Dysfunctional mitochondria would be less able to carry out the metabolism of fatty acids, leading to lipid accumulation in the setting of a high-fat diet.

Further research will be required to better define the physiological roles of both of these two positional candidate genes and to determine whether the amino acid differences detected between the LG/J and SM/J alleles are

indeed responsible for the observed QTL effect. These future studies will be based not on gene mapping but on functional evaluation of protein levels and activities associated with the variant alleles. In addition, other genes within or near the confidence region on proximal chromosome 13 will be similarly sequenced and analyzed.

ACKNOWLEDGMENTS

This work was supported by the National Institutes of Health (grants DK55736, DK52514, HL58427, and RR15116), the Washington University Clinical Nutrition Research Unit (DK56341), and the Washington University Diabetes Research Training Center (2 P60 DK20579).

REFERENCES

- Ravussin E, Bouchard C: Human genomics and obesity: finding appropriate drug targets. *Eur J Pharmacol* 410:131–145, 2000
- Yanovski JA, Yanovski SZ: Recent advances in basic obesity research. *JAMA* 282:1504–1506, 1999
- Seidell JC: Dietary fat and obesity: an epidemiologic perspective (Review). *Am J Clin Nutr* 67:546S–550S, 1998
- Sarkar S: From the *Reaktionsnorm* to the adaptive norm: the norm of reaction, 1909–1960. *Biology and Philosophy* 14:235–252, 1999
- Pigliucci M: *Phenotypic Plasticity: Beyond Nature and Nurture*. Baltimore, MD, Johns Hopkins University Press, 2001
- West-Eberhard MJ: *Developmental Plasticity and Evolution*. New York, Oxford University Press, 2003
- Finck BN, Han X, Courtois M, Aimond F, Nerbonne JM, Kovacs A, Gross RW, Kelly DP: A critical role for PPAR α -mediated lipotoxicity in the pathogenesis of diabetic cardiomyopathy: modulation by dietary fat content. *Proc Natl Acad Sci U S A* 100:1226–1231, 2003
- Weiss EP, Brown MD, Shuldiner AR, Hagberg JM: Fatty acid binding protein-2 gene variants and insulin resistance: gene and gene-environment interaction effects. *Physiol Genomics* 10:145–157, 2002
- Loomis WF, Sternberg PW: Genetic networks (Comment). *Science* 269:649, 1995
- Luan J, Browne PO, Harding AH, Halsall DJ, O'Rahilly S, Chatterjee VK, Wareham NJ: Evidence for gene-nutrient interaction at the PPAR γ locus. *Diabetes* 50:686–689, 2001
- Ordovas JM, Corella D, Demissie S, Cupples LA, Couture P, Coltell O, Wilson PW, Schaefer EJ, Tucker KL: Dietary fat intake determines the effect of a common polymorphism in the hepatic lipase gene promoter on high-density lipoprotein metabolism: evidence of a strong dose effect in this gene-nutrient interaction in the Framingham Study. *Circulation* 106:2315–2321, 2002
- Tai ES, Corella D, Deurenberg-Yap M, Cutter J, Chew SK, Tan CE, Ordovas JM: Dietary fat interacts with the -514C>T polymorphism in the hepatic lipase gene promoter on plasma lipid profiles in a multiethnic Asian population: the 1998 Singapore National Health Survey. *J Nutr* 133:3399–3408, 2003
- Todd JA, Farrall M: Panning for gold: genome-wide scanning for linkage in type 1 diabetes (Review). *Hum Mol Genet* 5:1443–1448, 1996
- Mokdad AH, Serdula MK, Dietz WH, Bowman BA, Marks JS, Koplan JP: The spread of the obesity epidemic in the United States, 1991–1998. *JAMA* 282:1519–1522, 1999
- Fisler JS, Warden CH: Mapping of mouse obesity genes: a generic approach to a complex trait (Review). *J Nutr* 127:1909S–1916S, 1997
- Chai C: Analysis of quantitative inheritance of body size in mice. I. Hybridization and maternal influence. *Genetics* 41:157–164, 1956
- Chai C: Analysis of quantitative inheritance of body size in mice. II. Gene action and segregation. *Genetics* 41:165–178, 1956
- Cheverud JM, Routman EJ, Duarte FA, van Swinderen B, Cothran K, Perel C: Quantitative trait loci for murine growth. *Genetics* 142:1305–1319, 1996
- Cheverud JM, Pletscher LS, Vaughn TT, Marshall B: Differential response to dietary fat in large (LG/J) and small (SM/J) inbred mouse strains. *Physiol Genomics* 1:33–39, 1999
- Ehrich TH, Kenney JP, Vaughn TT, Pletscher LS, Cheverud JM: Diet, obesity, and hyperglycemia in LG/J and SM/J mice. *Obes Res* 11:1400–1410, 2003
- Cheverud JM, Ehrich TH, Kenney JP, Pletscher LS, Semenovich CF: Genetic evidence for discordance between obesity and diabetes-related traits in the LGXSM recombinant inbred mouse strains. *Diabetes* 53:2700–2708, 2004
- Cheverud JM, Vaughn TT, Pletscher LS, Peripato AC, Adams ES, Erikson CF, King-Ellison KJ: Genetic architecture of adiposity in the cross of LG/J and SM/J inbred mice. *Mamm Genome* 12:3–12, 2001
- Darvasi A, Soller M: Advanced intercross lines, an experimental population for fine genetic mapping. *Genetics* 141:1199–1207, 1995
- MacArthur J: Genetics of body size and related characters. I. Selection of small and large races of the laboratory mouse. *Am Nat* 78:142–157, 1944
- Goodale H: A study of the inheritance of body weight in the albino mouse by selection. *J Hered* 29:101–112, 1938
- Dietrich WF, Miller J, Steen R, Merchant MA, Damron-Boles D, Husain Z, Dredge R, Daly MJ, Ingalls KA, O'Connor TJ: A comprehensive genetic map of the mouse genome. *Nature* 380:149–152, 1996
- Lander ES, Green P, Abrahamson J, Barlow A, Daly MJ, Lincoln SE, Newburg L: MAPMAKER: an interactive computer package for constructing primary genetic linkage maps of experimental and natural populations. *Genomics* 1:174–181, 1987
- Lincoln S, Daly M, Lander E: Constructing genetic maps with MAPMAKER/EXP 3.0. Boston, MA, Whitehead Institute, 1992
- Lander ES, Botstein D: Mapping mendelian factors underlying quantitative traits using RFLP linkage maps. *Genetics* 121:185–199, 1989 [published erratum appears in *Genetics* 136:705, 1994]
- Vaughn TT, Pletscher LS, Peripato A, King-Ellison K, Adams E, Erikson C, Cheverud JM: Mapping quantitative trait loci for murine growth: a closer look at genetic architecture. *Genet Res* 74:313–322, 1999
- Wilkinson L, Coward M: Linear models III: General linear models. In *SYSTAT 8.0: Statistics*. Chicago, SPSS, 1998, p. 457–516
- Cheverud JM: The genetic architecture of pleiotropic relations and differential epistasis. In *The Character Concept in Evolutionary Biology*. Wagner GP, Ed. San Diego, CA, Academic Press, 2001, p. 411–434
- Wilkinson L, Coward M: Linear Models II: Analysis of variance. In *SYSTAT 10: Statistics I*. Chicago, SPSS, 2000
- Haley CS, Knott SA: A simple regression method for mapping quantitative trait loci in line crosses using flanking markers. *Heredity* 69:315–324, 1992
- Ehrich TH: *QTL Analysis Package*. 4.01 ed. St. Louis, MO, 2004
- Wilkinson L, Engelman L, Marcantonio R: Correlations, similarities, and distance measures. In *SYSTAT 10: Statistics I*. Wilkinson L, Ed. Chicago, SPSS Science Marketing Department, 2000, p. 1-115–1-146
- Falconer DS, Mackay TFC: *Introduction to Quantitative Genetics*. 4th ed. New York, John Wiley and Sons, 1996
- Zeng ZB: Precision mapping of quantitative trait loci. *Genetics* 136:1457–1468, 1994
- Cheverud JM: A simple correction for multiple comparisons in interval mapping genome scans. *Heredity* 87:52–58, 2001
- Ng PC, Henikoff S: Predicting deleterious amino acid substitutions. *Genome Res* 11:863–874, 2001
- Thompson JD, Higgins DG, Gibson TJ: CLUSTAL W: improving the sensitivity of progressive multiple sequence alignment through sequence weighting, position-specific gap penalties and weight matrix choice. *Nucleic Acid Res* 22:4673–4680, 1996
- Gunasekera D, Kemp RG: Cloning, sequencing, expression, and purification of the C isozyme of mouse phosphofructokinase. *Protein Expr Purif* 16:448–453, 1999
- Martinez-Costa OH, Hermida C, Sanchez-Martinez C, Santamaria B, Aragon JJ: Identification of C-terminal motifs responsible for transmission of inhibition by ATP of mammalian phosphofructokinase, and their contribution to other allosteric effects. *Biochem J* 377:77–84, 2004
- Sanchez-Martinez C, Estevez AM, Aragon JJ: Phosphofructokinase C isozyme from ascites tumor cells: cloning, expression, and properties. *Biochem Biophys Res Commun* 271:635–640, 2000
- Goldstein BJ, Scalia R: Adiponectin: a novel adipokine linking adipocytes and vascular function. *J Clin Endocrinol Metab* 89:2563–2568, 2004
- Browning JD, Horton JD: Molecular mediators of hepatic steatosis and liver injury. *J Clin Invest* 114:147–152, 2004
- Gayles EC, Pagliasotti MJ, Prach PA, Koppenhafer TA, Hill JO: Contribution of energy intake and tissue enzymatic profile to body weight gain in high-fat-fed rats. *Am J Physiol* 272:R188–R194, 1997
- Patti ME, Butte AJ, Crunkhorn S, Cusi K, Berria R, Kashyap S, Miyazaki Y, Kohane I, Costello M, Saccone R, Landaker EJ, Goldfine AB, Mun E, DeFronzo R, Finlayson J, Kahn CR, Mandarino LJ: Coordinated reduction of genes of oxidative metabolism in humans with insulin resistance and diabetes: potential role of PGC1 and NRF1. *Proc Natl Acad Sci U S A* 100:8466–8471, 2003
- Petersen KF, Dufour S, Befroy D, Garcia R, Shulman GI: Impaired mitochondrial activity in the insulin-resistant offspring of patients with type 2 diabetes. *N Engl J Med* 350:664–671, 2004
- Taylor R: Causation of type 2 diabetes: the Gordian knot unravels. *N Engl J Med* 350:639–641, 2004
- Lowell BB, Shulman GI: Mitochondrial dysfunction and type 2 diabetes. *Science* 307:384–387, 2005